Interaction of Silver, Cesium, and Zinc with Alumina Surfaces: Thermal Desorption and Photoemission Studies

José A. Rodriguez,* Mark Kuhn, and Jan Hrbek

Chemistry Department, Brookhaven National Laboratory, Upton, New York 11973

Received: July 22, 1997; In Final Form: September 16, 1996[⊗]

Cs, Ag, and Zn behave in a different way when deposited on surfaces of ultrathin (15−20 Å) films of alumina. In the case of Cs/Al_2O_3, the alkali atoms wet the oxide, forming strong chemisorption bonds. At small coverages of Cs, desorption of the alkali occurred between 600 and 1000 K. As the amount of Cs deposited increased, there was a reduction in the Cs desorption temperature to ∼350 K. This broad range of desorption temperatures reflects a continuous decrease in the Cs adsorption energy from 63 to 18 kcal/mol with increasing Cs coverage. The deposition of small amounts of Cs induced large (0.9−1.1 eV) positive shifts in the binding energies of the O KVV, O 1s, and Al 2p features of the alumina films. This is consistent with a transfer of electrons from Cs into surface states of alumina that produces a transformation similar to a change from p-type to n-type semiconductors. Ag and Zn do not wet the surface of alumina well and form three-dimensional clusters or particles. In these systems, the activation energies for desorption of the admetal increase with cluster size (20 kcal/mol for Ag, 10 kcal/mol for Zn). The deposition of Ag and Zn induces only minor perturbations in the electronic properties of alumina. Small silver clusters supported on alumina exhibit an incompletely developed metallic band structure. The differences in the behavior of the Cs/Al_2O_3 and Ag/Al_2O_3 or Zn/Al_2O_3 systems are explained in terms of variations in the surface free energy of the admetals and in the nature of the admetal−oxide bonds.

I. Introduction

Most commercial catalysts consist of small metal particles supported on high-surface-area oxides.[1,2] In these systems, the oxide may behave as an inert support or may actually modify the activity of the metal catalyst.[1,2] Metal particles or adlayers on oxide surfaces are also relevant to crystal growth, gas sensor operation, bonding in composites, and the fabrication of devices in the microelectronics industry.[3] Despite these technologically important applications, our understanding of the behavior of metal/oxide interfaces is rather rudimentary.[4] This fact has motivated many studies investigating the interaction of metals with oxide surfaces in recent years.[3−17]

The growth of metals on alumina surfaces has received considerable attention.[5,7,12,17] Studies for the deposition of Pt,[17c] Rh,[17b] Cu,[5a,f] and Ag[10a] on α-$Al_2O_3(0001)$ and Ag on α-$Al_2O_3(11\bar{2}0)$[10] show poor wetting of the alumina surfaces by the admetals at 300 K. In all these systems, the admetal grows, forming three-dimensional (3D) islands or clusters (Volmer−Weber growth mode).[5,10,17] For the deposition of Pd on α-$Al_2O_3(0001)$ at 300 K, a layer-by-layer rise (Frank−Van der Merwe growth mode) of the metal film has been observed.[17a] The Pd film coalesces into 3D particles upon heating to temperatures above 600 K.[17a] X-ray photoelectron spectra for Pt particles supported on α-$Al_2O_3(0001)$ show positive binding-energy shifts (0.3−0.4 eV) in the Pt 4f core levels.[7b,12a] Small Pt particles exhibit an incompletely developed metallic band structure.[12a] In general, the reactivity of alumina-supported Rh, Pd, and Pt particles toward small molecules (H_2, CO, NO, etc.) depends strongly on the size of the particles.[5,17]

In this article, we examine the interaction of silver, cesium, and zinc with alumina surfaces using thermal desorption mass spectroscopy (TDS) and core- and valence-level photoemission. Our interest in the Ag/Al_2O_3 and Cs/Al_2O_3 systems in part originates in the relevance that they have for the catalytic synthesis of ethylene epoxide. The oxidation of ethylene to ethylene epoxide ($2C_2H_4 + O_2 \rightarrow 2C_2H_4O$) is a several billion dollar per year industry.[18] The most common catalyst consists of reduced silver particles dispersed on α-alumina with cesium added as a promoter.[1,18] By studying the adsorption of Ag, Cs, and Zn on alumina, we deal with admetals that can form oxides with a large range of thermal stabilities:[19] Ag_2O, $\Delta H_f = -7.3$ kcal/mol; Cs_2O, $\Delta H_f = -75.9$ kcal/mol; Cs_2O_2, $\Delta H_f = -96.2$ kcal/mol; ZnO, $\Delta H_f = -83.2$ kcal/mol. Cesium and zinc have a much larger affinity toward oxygen than any of the admetals (Cu, Rh, Pd, Ag, Pt) studied in previous work.

Surface science studies of many oxides have been hindered by surface charging effects.[3] Thin oxide films grown on a metallic substrate represent an attractive model system where the surface charging problem is eliminated.[5,9,20,21] Electrons can tunnel through the insulating film into a metal surface, thus allowing an exploitation of surface sensitive techniques where either electrons or ions are used.[5a,9,20] It has been shown that ultrathin (5−20 Å) films of Al_2O_3 can be grown on a Mo(110) substrate.[5f,21] In this work, we use these films to investigate the interaction of Ag, Cs, and Zn with alumina. Previous studies carried out in our laboratory show identical adsorption/desorption behavior of Ag on the oxide films and on a α-$Al_2O_3(11\bar{2}0)$ single crystal, indicating that the films are a viable model for an α-alumina support.[10b]

II. Experimental Methods

II.1. Instrumentation. The experiments were carried out in a conventional ultrahigh vacuum system (base pressure $\approx 3 \times 10^{-10}$ Torr) equipped with instrumentation for TDS, photoemission, and ion-scattering spectroscopy (ISS). The photoemission spectra reported in section III were acquired using unmonochromatized Mg Kα radiation and a hemispherical electron energy analyzer with multichannel detection. In order to enhance surface sensitivity, the sample was positioned such that

* To whom correspondence should be addressed.

[⊗] Abstract published in *Advance ACS Abstracts,* November 1, 1996.

S0022-3654(96)02195-8 CCC: $12.00

the takeoff angle for electron detection was 30° off normal. The binding-energy scale for the photoemission spectra was calibrated by setting the Zn $2p_{1/2}$, Cs $3d_{5/2}$, and Ag $3d_{5/2}$ core levels of the pure metals to binding energies of 1044.9, 726.6, and 368.0 eV, respectively.[22] The experiments of ISS were performed using He^+ as the incident ion and using a scattering angle of 90°. TDS measurements were carried out using a quadrupole mass spectrometer, which was housed in a differentially pumped liquid-nitrogen-cooled jacket that had a small aperture in the front. In this arrangement, the mass spectrometer detected only species that desorbed from the "front" face of the sample during the thermal desorption experiments.

The Mo(110) substrate was mounted on a manipulator capable of liquid-nitrogen cooling to 80 K and resistive heating to 1550 K. An electron-beam assembly provided the capability for heating to 2500 K. Temperatures were monitored with a (W−5% Re)/(W−26% Re) thermocouple spot-welded to the upper edge of the Mo(110) crystal. The crystal was cleaned according to standard procedures.[23] The cleanliness of the surface was verified by means of X-ray photoelectron spectroscopy (XPS).

II.2. Preparation of Alumina Films. We followed two different routes to prepare the alumina films, and both produced films of the same quality as judged by the results of XPS, ISS, and the adsorption/desorption of Ag, Cs, and Zn. In the first procedure, aluminum atoms (generated by heating a W filament wrapped with a high-purity wire of Al) were dosed to the Mo(110) substrate in a background O_2 pressure of 10^{-5}−10^{-6} Torr, with subsequent annealing to 1200 K to improve the crystalline quality of the film. This methodology has been used by several authors to grow ultrathin Al_2O_3 films on Mo(110)[5f,21] and other metal substrates.[5a,24]

In the second procedure, the Mo(110) substrate was initially exposed to NO_2 (5−50 L) at 950−1000 K and ultrathin films of molybdenum oxide were formed through the reaction: $NO_{2,gas} + Mo \rightarrow N_{2,gas} + MoO_x$. Then Al was vapor deposited on the molybdenum oxide film at 700 K and alumina was produced ($Al + MoO_x \rightarrow AlO_x + Mo$). This was followed by annealing to 1200 K in ambient oxygen (10^{-7} Torr) for 2−5 min. The results of He-ISS spectra indicated that no Mo was present in the surface of these films, and the attenuation of the Mo 3d signal in XPS spectra pointed toward an epitaxial growth of alumina on the molybdenum substrate.[5,24] The alumina films exhibited an O 1s peak in the range 532.1−532.4 eV and a binding-energy shift of 2.6−2.9 eV in the Al 2p features (for a typical result, see Figure 1). These are strong indications of the formation of stoichiometric Al_2O_3.[24,25]

The experiments described in section III were carried out over alumina films that were 15−20 Å thick (as determined from the intensity of the Mo 3d and Al 2p signals in the corresponding XPS spectra[5a,24]).

II.3. Admetal Deposition. Silver and zinc were deposited by sublimation from high-purity wires of Ag and Zn, which were heated by W filaments. The atomic flux from the metal dosers was calibrated according to the methodology described in our previous studies for Ag/Mo(110)[26] and Zn/Mo(110).[27] In this work, the amount of Ag or Zn dosed is reported with respect to the number of Mo(110) surface atoms. One equivalent monolayer (ML) of the admetal corresponds to the deposition of 1.43×10^{15} atoms cm^{-2} of Ag or Zn. Cesium was vapor-deposited from a SAES getter chromate source. The metal dosers were outgassed thoroughly prior to vapor deposition.

III. Results

III.1. Interaction of Silver and Alumina. On clean Mo(110) at 300 K, silver grows layer-by-layer.[28] The corresponding TDS spectra display Ag desorption temperatures that increase from 1020 to 1075 K when the Ag coverage is raised from 0.2 to 1.0 ML.[26] For Ag multilayers deposited on clean Mo(110), the onset of desorption appears at ∼850 K.[26] Figure 2 shows Ag thermal desorption spectra acquired after depositing silver at 300 K on an alumina film (bottom panel) and on a Mo(110) surface covered with a saturated layer of chemisorbed oxygen[29] (top panel). The TDS results for Ag/O/Mo(110) surfaces indicate that the oxygen overlayer prevents the formation of Mo−Ag bonds. The Ag desorption features from O/Mo(110) match well those seen for Ag multilayers on clean Mo(110) or other metal substrates, with a common leading edge and a line shape typical of zero-order desorption kinetics. This behavior is consistent with the formation of large 3D clusters or islands of silver on the O/Mo(110) surface.

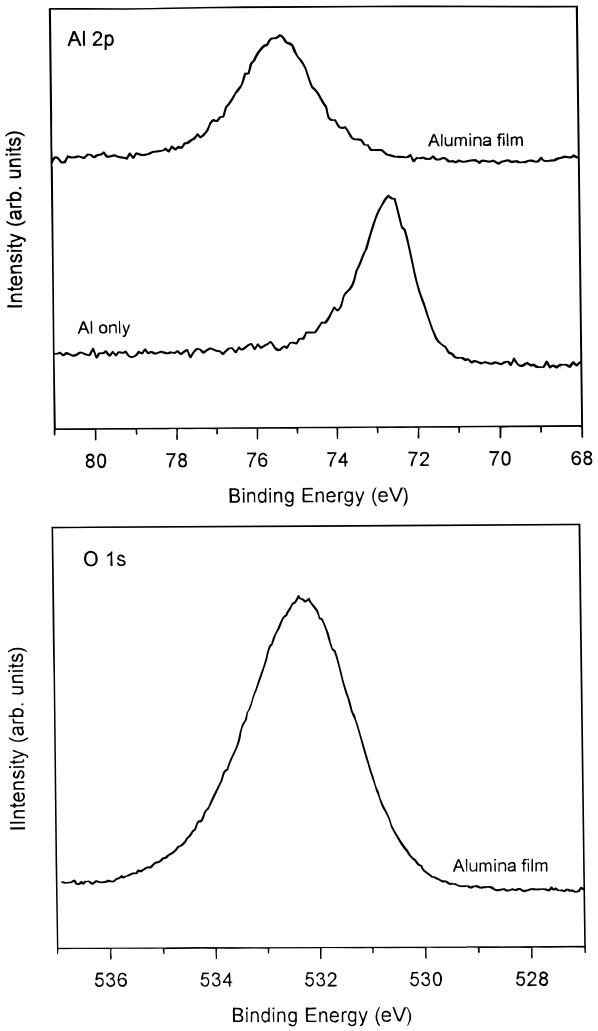

Figure 1. Al 2p (top) and O 1s (bottom) XPS spectra for an ultrathin (∼20 Å) alumina film. In the top part of the figure, for comparison, we also include the Al 2p spectrum of a film (>25 Å) of metallic aluminum.

In Figure 2, the desorption of silver from the alumina film occurs between 800 and 1000 K. The Ag desorption features do not show the common leading edge expected for zero-order desorption kinetics. This is very clear at low coverages of the admetal, where there is a shift toward higher temperature in the complete Ag desorption peak as the Ag coverage increases. An identical phenomenon was observed in spectra for the desorption of silver from alumina films supported on Ru(001) and an α-$Al_2O_3(11\bar{2}0)$ single crystal.[10b] A complete analysis of these Ag desorption data[10b] yielded activation energies for desorption (30−60 kcal/mol) that were smaller than the heat of

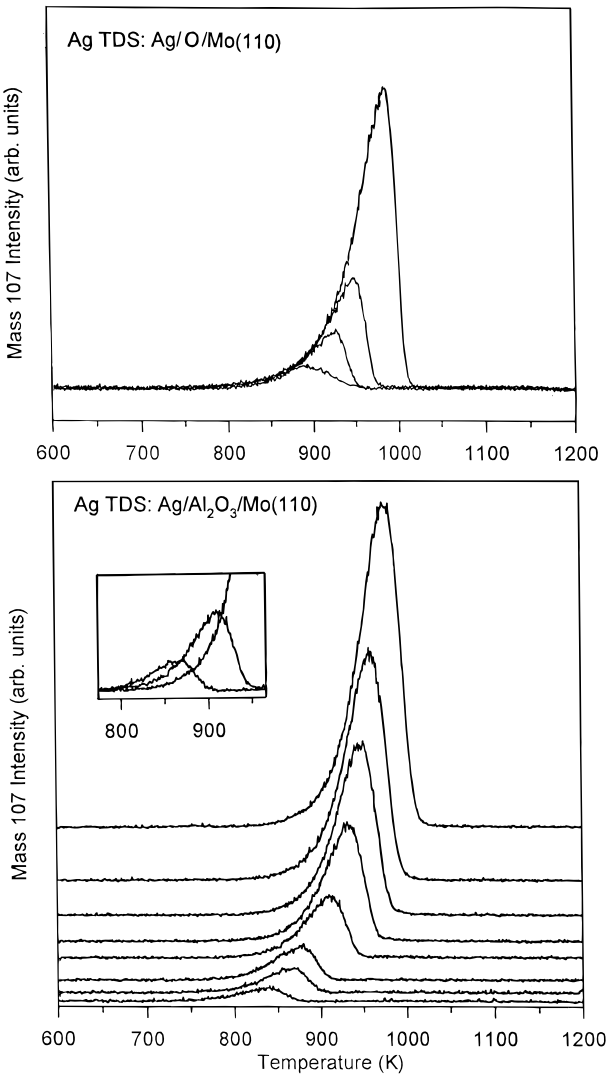

Figure 2. Top: Ag thermal desorption spectra acquired after depositing silver on a O/Mo(110) surface (θ_O = saturation). The spectra correspond to Ag coverages of 0.21, 0.63, 1.28, and 3.43 ML. Bottom: Ag thermal desorption spectra acquired after depositing silver on an ultrathin (∼20 Å) alumina film supported on Mo(110). The spectra correspond to silver coverages of 0.14, 0.26, 0.37, 0.70, 1.35, 1.91, 2.57, and 3.64 ML. The inset compares the desorption spectra for 0.26, 0.70, and 3.64 ML of silver. Heating rate = 5 K/s.

sublimation of silver (68 kcal/mol) and yielded a fractional order (0.6−0.8) for the dependence of the desorption rate on Ag coverage. The trends seen in Figure 2 for the desorption of Ag from alumina are in good agreement with trends found in Monte Carlo simulations for the desorption of islands (or particles) from a surface.[30] Small particles will desorb more easily than "infinite" particles owing to differences in surface tension.[30] An atom at the edge of a small island has fewer nearest neighbors than in the bulk of an "infinite" island, so it desorbs more easily than the atoms in an "infinite" island".[5a,10b,30] As a result, the TDS peaks shift to lower temperatures with decreasing coverage when small islands are formed.[30] The TDS data in Figure 2 indicate that the 3D clusters formed after depositing Ag on the O/Mo(110) surface are of bigger size than those formed on the alumina film. One can reach an identical conclusion after examining the results of XPS experiments.

Figure 3 shows Ag 3d XPS spectra recorded after depositing 1.3 ML of Ag on the alumina film used to obtain the TDS data in Figure 2. Annealing from 330 to 700 K (close to the onset of silver desorption) leads only to minor changes (<10%) in the intensity and position of the Ag 3d peaks. This indicates

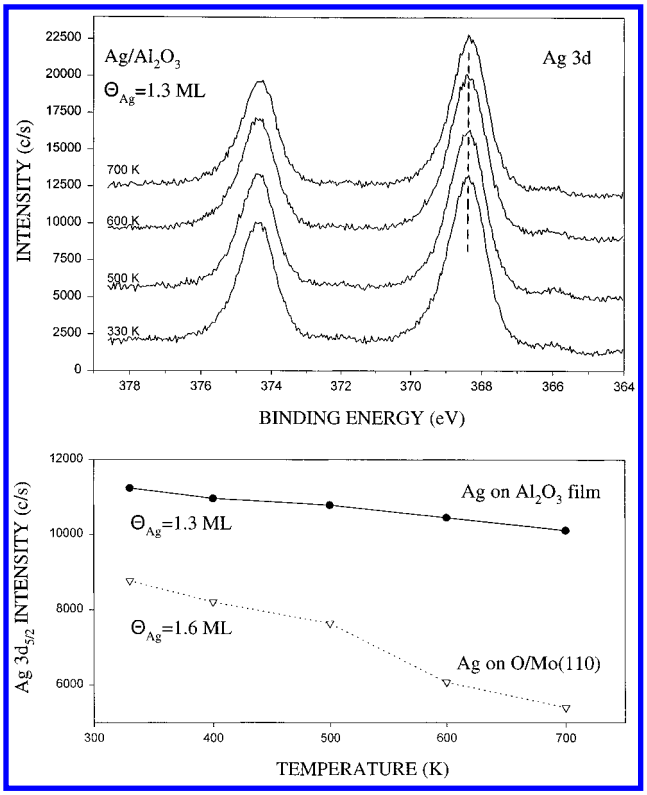

Figure 3. Top: Ag 3d XPS spectra acquired after dosing 1.3 ML of silver on an ultrathin (∼20 Å) alumina film at 330 K with subsequent annealing (60 s) to 500, 600, and 700 K. Bottom: Effect of temperature on the Ag $3d_{5/2}$ intensity of $Ag_{1.3}$/alumina and $Ag_{1.6}$/O/Mo(110) surfaces.

that the small Ag clusters formed at 330 K[10] are neither diffusing into the bulk of the alumina substrate nor forming large 3D particles upon heating (i.e., sintering). For the deposition of 1.6 ML of Ag on the O/Mo(110) surface, one finds a Ag 3d intensity smaller than that seen after depositing 1.3 ML of Ag on the alumina film, and the silver signal in the Ag/O/Mo(110) system decreases considerably (∼40%) after heating from 330 to 700 K (see bottom of Figure 3). These results are consistent with the formation of large 3D clusters of silver on the O/Mo(110) surface. Therefore, it is not surprising that the Ag/O/Mo(110) and Ag/alumina systems show a different behavior in TDS experiments.

Figures 4 and 5 display core- and valence-level photoemission spectra acquired after depositing several coverages of silver on an alumina film at ∼300 K. A surface with 0.3 ML of silver exhibits Ag 3d peak positions that are shifted ∼0.6 toward higher binding energy with respect to those of bulk metallic Ag (374.0 and 368.0 eV[22]). As the silver coverage increases, there is a monotonic decrease in the Ag 3d binding energies until the values for pure Ag are reached at θ_{Ag} = 9.1 ML. Similar negative binding-energy shifts were observed in the centroid of the Ag 4d band and in the Ag MVV Auger transition (not shown). The binding-energy shifts in Figure 4 cannot be attributed to the formation of Ag−O bonds, since the Ag 3d core levels of Ag_2O and AgO appear 0.4−0.7 eV at lower binding energies than those of metallic Ag.[31] Ag atoms deposited on Al(100)[32] show binding-energy shifts similar to those in Figure 4, but the Ag desorption temperatures in Figure 2 are not consistent with the possible presence of Ag−Al bonds. Thus, the binding-energy shifts in Figure 4 probably come from changes in final-state relaxation energy.[33] In a "bulk" metal the screening of the photoemission core-hole is more effective than in an oxide or small metal particles.[33] Therefore, when the Ag coverage increases in the Ag/alumina systems, there is

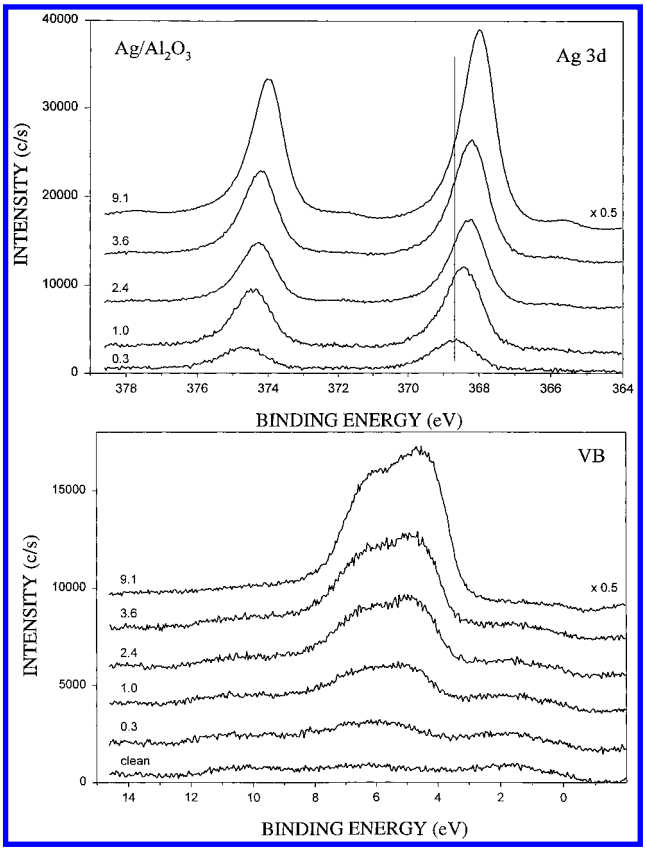

Figure 4. Photoemission spectra for the Ag 3d (top) and valence (bottom) regions of Ag/alumina surfaces (θ_{Ag} = 0.3, 1.0, 2.4, 3.6, and 9.1 ML). The deposition of silver and acquisition of the spectra were carried out at ~300 K. The electrons were excited using Mg Kα radiation.

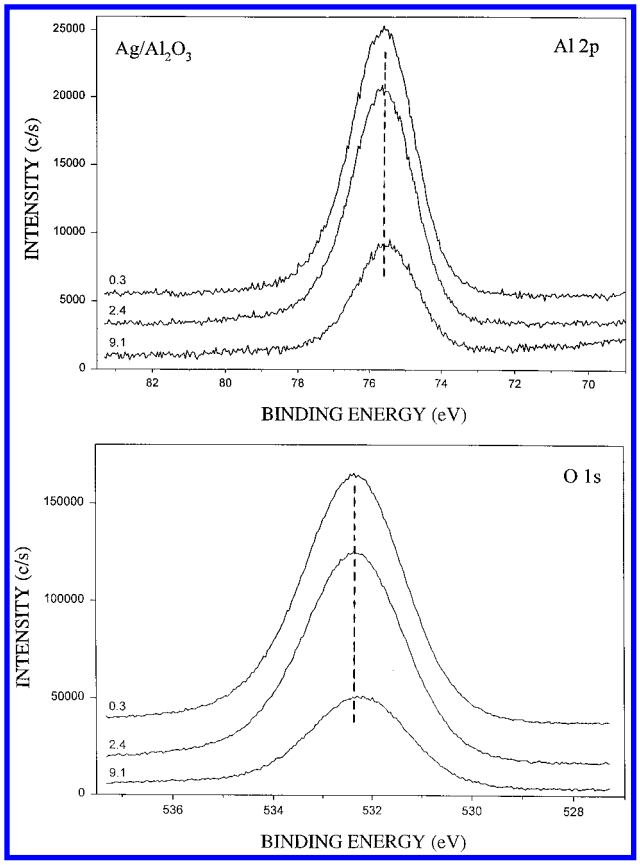

Figure 5. Al 2p and O 1s XPS spectra acquired in the same set of experiments that led to the Ag 3d and valence spectra in Figure 4. The coverage of Ag in the Ag/alumina systems was 0.3, 2.4, and 9.1 ML.

an "apparent" shift toward lower binding energy in the Ag 3d levels and 4d band.

In the bottom of Figure 4, we can see valence band spectra for a series of Ag/alumina surfaces. Since the valence region was examined using Mg Kα radiation, the intensity of electron emissions from the alumina bands is very weak, and the valence spectra are dominated by electron emissions from the Ag bands. For a surface with 0.3 ML of Ag, emissions from the Ag 4d band appear from 4.5 to 7.5 eV, with a band centroid located around 6 eV. This is very different from the band structure of metallic Ag,[34] where the 4d band extends from 3 to 8 eV and is dominated by a strong peak at ~4.5 eV. As the Ag coverage increases in Figure 4, the band structure of the supported Ag clusters evolves toward that of bulk Ag. There is a clear rise in the density of states in the 4.0−4.5 eV region, and the full-width at half-maximum of the 4d band increases from 2.4 eV at 0.3 ML to 2.9 eV at 1.0 ML and finally to 3.3 eV at 9.1 ML.

Figure 5 illustrates how the Al 2p and O 1s core levels of an alumina film change after the adsorption of silver. The deposition of 0.3 ML of Ag induced negligible changes in the position and intensity of the Al 2p and O 1s peaks of the film. For a film with 2.4 ML of Ag, there is a reduction of ~15% in the intensity of the Al 2p and O 1s features (without significant changes in peak positions). This small reduction is consistent with the formation of 3D clusters of Ag on top of the alumina film. After depositing 9.1 ML of Ag, one sees a large attenuation in the Al 2p and O 1s signals with very small (0.10−0.15 eV) negative binding-energy shifts, which can be attributed to an increase in the final-state relaxation energy within the escape depth probed by XPS.[33]

III.2. Interaction of Cesium and Alumina. In general, cesium shows a much larger affinity toward oxygen than silver,[35] forming oxides with a much bigger thermal stability (Ag_2O, $\Delta H_f = -7.3$ kcal/mol; Cs_2O, $\Delta H_f = -75.9$ kcal/mol[19]). This leads to very important differences in the nature of the Ag ↔ Al_2O_3 and Cs ↔ Al_2O_3 interactions.

Figure 6 shows thermal desorption spectra taken after adsorbing different amounts of cesium on an ultrathin (~20 Å) alumina film at 80 K. XPS spectra indicated that no cesium was left on the alumina after heating to 1100 K. At small doses of Cs desorption of the alkali occurred between 600 and 1000 K. As the amount of cesium deposited increased, there was a large reduction in the cesium desorption temperature. The Cs desorption peak at ~320 K grew continuously without saturation and agrees well with the desorption temperature observed in previous studies of cesium multilayers.[36] On the other hand, the Cs desorption features between 400 and 1000 K can be assigned to the desorption of Cs atoms that were strongly bound to the alumina. The broad range of desorption temperatures seen in Figure 6 reflects a continuous decrease in the Cs adsorption energy from 63 to 18 kcal/mol.[37] A similar phenomenon has been reported for the adsorption of Cs on metal surfaces[36] and on $TiO_2(110)$[4a,38] and has been attributed to a reduction in the ionicity of the Cs−substrate bond with increasing Cs coverage due to dipole−dipole repulsion.[4,39] TDS spectra acquired during the decomposition of CsO_x films show desorption of cesium at temperatures from 700 to 1000 K.[40] Thus, in Figure 6, the Cs desorption features between 700 and 1000 K could come from the decomposition of oxide compounds in which Cs is sharing O atoms with Al.

Figure 7 displays photoemission spectra recorded after depositing cesium on an alumina film at 80 K. In the top panel of the figure, we can see the O KVV Auger transition for alumina (755−735 eV region) and the 3d peaks for cesium (755−723 eV region). In the Cs 3d spectrum of the cesium

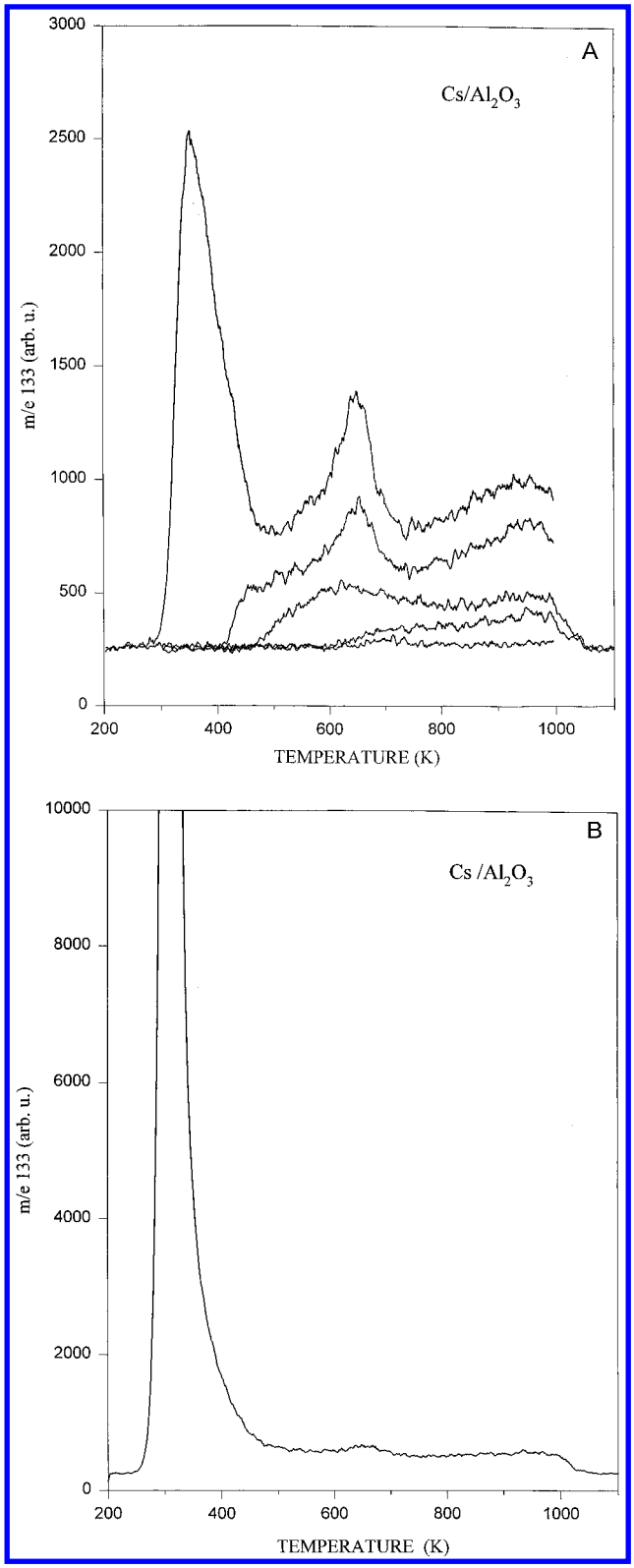

Figure 6. Cesium thermal desorption spectra acquired after depositing small (part A) or large (part B) amounts of Cs on an ultrathin (~20 Å) alumina film at 80 K. Heating rate = 5 K/s.

multilayer, the two sharp peaks at 726.6 and 740.5 eV are the main 3d levels whereas the broad shoulders toward higher binding energy correspond to plasmon losses.[39,41] A direct comparison of the Cs 3d peak positions for the Cs multilayer and Cs atoms bonded to alumina is ambiguous owing to changes in the final-state relaxation energy. However, it is clear that the Cs $3d_{5/2}$ spectra in Figure 7 for the submonolayer Cs/alumina systems do not show a plasmon structure. Thus, we can

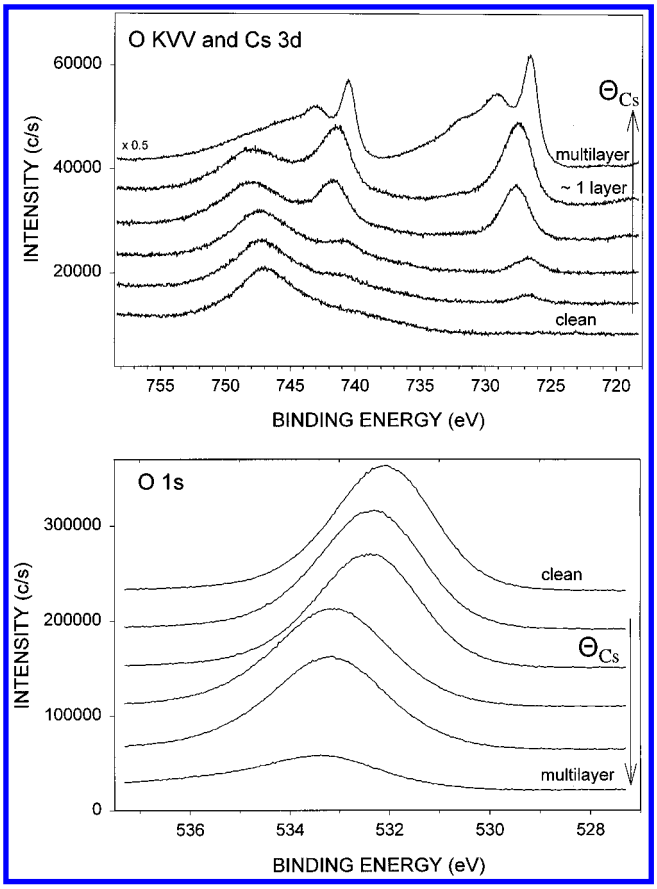

Figure 7. O KVV, Cs 3d, and O 1s photoemission spectra taken after depositing cesium on an ultrathin (~15 Å) alumina film at 80 K. The electrons were excited using Mg Kα radiation.

conclude that the Cs atoms bonded to alumina are not in a metallic state. The deposition of small amounts of Cs induced large (0.9−1.1 eV) positive shifts in the binding energies of the O KVV (Figure 7), O 1s (Figure 7), and Al 2p (not shown) features of the alumina film. In Figure 7, as the Cs coverage increases in the Cs/alumina systems, there is a simultaneous and almost identical shift in the O KVV, Cs 3d, and O 1s levels toward higher binding energy. This may be a consequence of changes in the Fermi level of the film within the bandgap due to the transfer of electrons from Cs into surface states of alumina. Similar binding-energy shifts are observed when doping semiconductors and switching from p-type to n-type materials.[33] To induce this transformation, only small concentrations of the doping agent are necessary.[33]

Figure 8 shows photoemission spectra acquired after annealing an alumina film covered with a cesium multilayer from 80 to 1200 K. Heating to 350 K induces the desorption of the Cs multilayer, and only Cs atoms that are bonded to alumina are left on the sample (see Figure 6). At this point the Cs $3d_{5/2}$ peak is broad, indicating that more than one type of Cs species is present on the surface. Further heating to 1000 K leads to desorption of most of the Cs, with subsequent large negative shifts in the binding energy of the O KVV, O 1s (not shown), Al 2p, and Cs 3d features. Upon annealing to 1200 K, all the cesium has desorbed, and the Al 2p, O 1s and O KVV spectra are now very similar to those obtained for the alumina film before the deposition of cesium.

The results in this section indicate the Cs ↔ Al_2O_3 interactions are much stronger than the Ag ↔ Al_2O_3 interactions, as can be expected from the difference in the thermal stability of cesium−oxygen and silver−oxygen compounds.[19] Cesium wets alumina

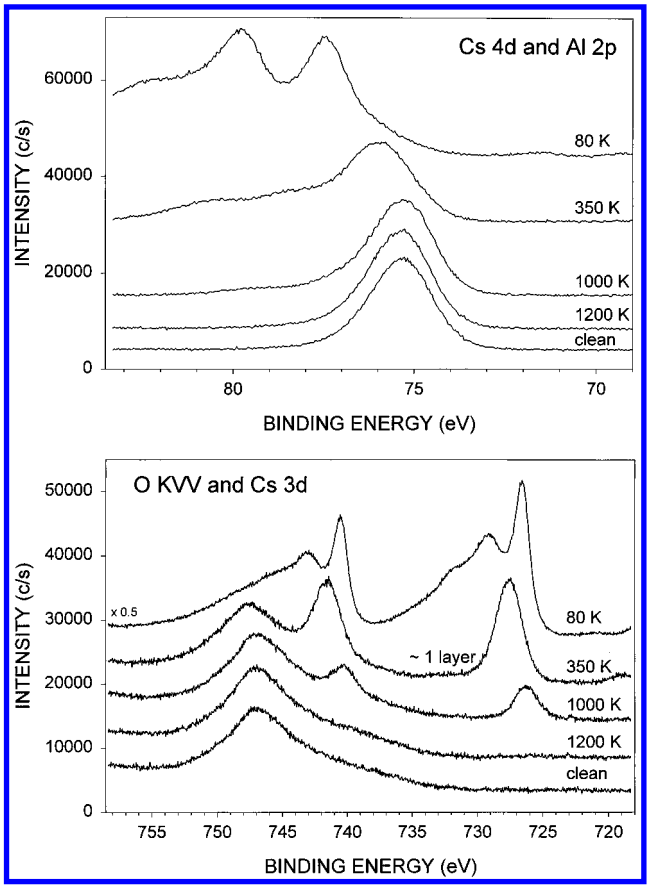

Figure 8. Auger and XPS spectra for Cs/alumina surfaces as a function of annealing temperature. In the first step, a Cs multilayer (>20 Å) was deposited on an ultrathin (~15 Å) alumina film at 80 K. This was followed by annealing to 350, 1000, and 1200 K. For comparison, we also include the Al 2p (top panel) and O KVV (bottom panel) spectra of the clean alumina film.

surfaces and induces large changes in the electronic properties of the oxide.

III.3. Interaction of Zinc and Alumina. Zinc forms oxides that exhibit a thermal stability comparable to that of cesium oxides.[42] However, the Zn ↔ Al_2O_3 interactions are much weaker than the Cs ↔ Al_2O_3 *and* Ag ↔ Al_2O_3 interactions. For example, the sticking coefficient of silver on alumina films and on a α-$Al_2O_3(11\bar{2}0)$ surface is close to 0.85 at 300 K.[10b] At this temperature, we were *unable* to adsorb zinc on alumina films supported on Mo(110). Significant sticking of zinc to the oxide surfaces was seen only when the temperature of the sample was below 250 K. Cadmium, like zinc, has a low sticking probability on oxides at room temperature.[11a]

Figure 9 shows zinc thermal desorption spectra acquired after exposing an ultrathin (~20 Å) alumina film to Zn atoms at 80 K. Evolution of Zn into the gas phase is observed at temperatures between 330 and 470 K. These desorption temperatures are much smaller than those seen for the decomposition of ZnO_x films (700−1000 K)[43] or the desorption of Zn from transition-metal surfaces (600−900 K).[44] The qualitative trends in Figure 9 are similar to the trends seen in Figure 2 for the desorption of silver from alumina: with increasing coverage of the admetal, there is a shift of the entire desorption peak toward higher temperature. This indicates that at low coverages Zn is forming small 3D clusters on alumina. The larger the cluster, the bigger the energy required to remove a Zn atom. In Figure 9, the activation energy for desorption of Zn varies from 23 kcal/mol at θ_{Zn} = 0.3 ML to 27 kcal/mol at θ_{Zn} = 4.2 ML.[45] These values are smaller than the heat of sublimation of metallic zinc (29 kcal/mol[19]).

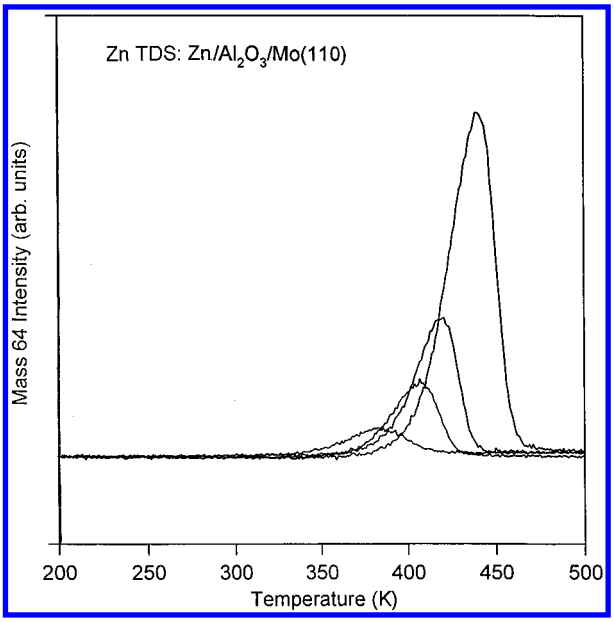

Figure 9. Zinc thermal desorption spectra acquired after depositing Zn on an alumina film at 80 K. The coverages of Zn are 0.3, 0.8, 1.7, and 4.2 ML. Heating rate = 5 K/s.

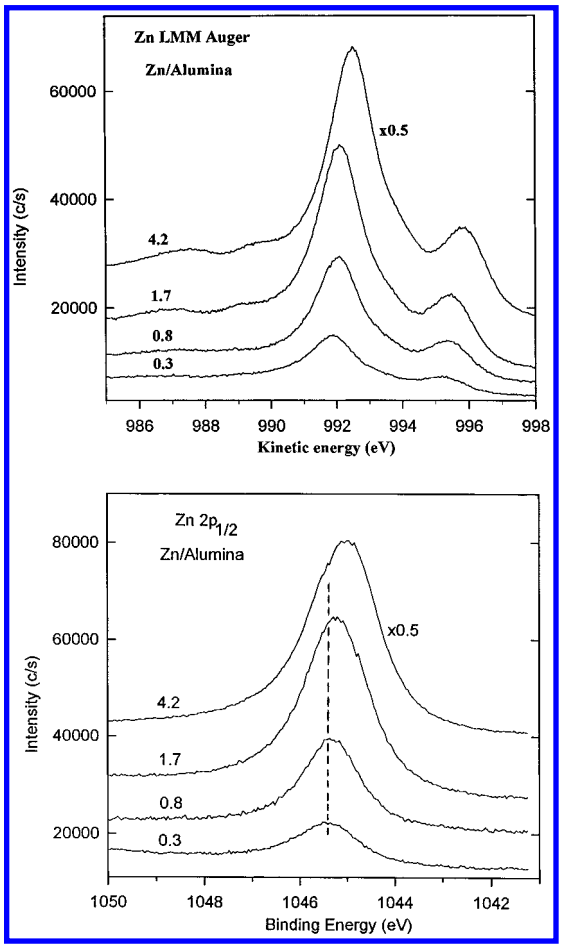

Figure 10. Zn LMM Auger and Zn $2p_{1/2}$ XPS spectra taken after depositing zinc on an ultrathin (~20 Å) alumina film at 80 K. The coverages of Zn in these Zn/alumina surfaces were 0.3, 0.8, 1.7, and 4.2 ML. The electrons were excited using Mg Kα radiation.

The results of photoemission experiments also indicate that the Zn ↔ Al_2O_3 interactions are relatively weak. Figure 10 displays Zn LMM Auger and Zn $2p_{1/2}$ XPS spectra for a series of Zn/alumina surfaces. The deposition of Zn and acquisition of the spectra were performed at 80 K. In the Zn $2p_{1/2}$ spectra,

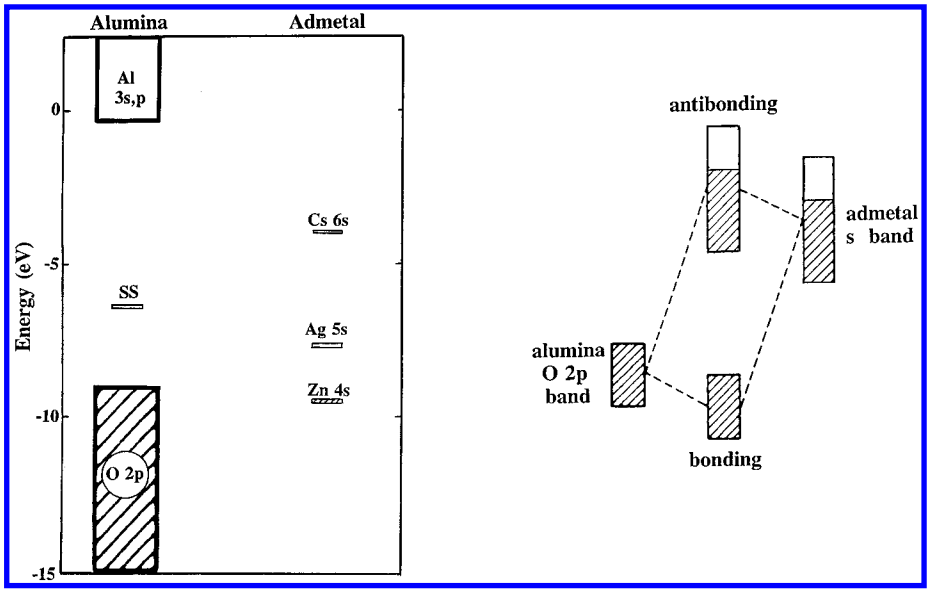

Figure 11. Left: Energy positions for the bands of alumina[53] and the valence s orbitals of atomic Cs, Ag, and Zn.[54] The energies are reported with respect to the vacuum level. The hatched areas denote fully occupied states or bands. For atomic Zn the 4s shell is completely filled, whereas the Ag(5s) and Cs(6s) shells are only half occupied. The label "SS" refers to surface states in alumina.[53] Right: Interaction between the O 2p band of alumina and the valence s band of Cs, Ag, and Zn adlayers.

there is a binding-energy shift of about −0.5 eV when the Zn coverage is increased from 0.3 to 4.2 ML. The spectrum for $\theta_{Zn} = 4.2$ ML exhibits a peak position (1045.0 eV) that is close to that of bulk metallic Zn (1044.9 eV[22]). The binding-energy shifts in the Zn $2p_{1/2}$ spectra could be attributed to the formation of ZnO_x at low coverages of the admetal.[46] However, this hypothesis can be ruled out on the basis of the peak positions seen in the Zn LMM spectra of Figure 10. In zinc oxides the Zn $L_3M_{45}M_{45}$ features appear at a kinetic energy of ∼988 eV[47,48] whereas for the Zn/alumina surfaces these features appear between 992 and 993 eV. Thus, the binding-energy shifts in Figure 10 probably come from changes in the final-state relaxation energy that accompany the growth of metal clusters and/or an oxide(insulator)-to-metal(conductor) transition within the escape depth probed by XPS.[33] The adsorption of zinc induced only very minor (<0.1 eV) negative shifts in the position of the Al 2p and O 1s peaks of the alumina substrate. The behavior seen for the Zn/alumina surfaces is similar in many aspects to that found for the Ag/alumina surfaces, where the admetal wets the alumina substrate poorly and has, therefore, only a minor influence on the electronic properties of the oxide.

IV. Discussion

The data presented above for the cesium/alumina systems indicate that the alkali atoms wet the oxide, forming strong chemisorption bonds. Studies examining the adsorption of alkalis on TiO_2, Cr_2O_3, and ZnO show that the alkali atoms spread out on the surface of these oxides, occupying in many cases specific sites offered by the oxide lattice.[4,9,49,50] For the interaction of alkalis with single-crystal faces of oxides, well-ordered overlayers have been observed.[4] For example, STM images for Na deposited on TiO_2(110) show a dispersed adlayer that forms p (4 × 2) and c (4 × 2) structures with increasing alkali coverage.[9b,50] These structures are a consequence of repulsive forces between the alkali adatoms.[4,9b] Up to relatively high coverages of the admetal, one can expect a shift (or polarization) of electron density from the alkali atoms toward the oxide substrate.[4,49a] To minimize dipole ↔ dipole repulsion, the alkali adatoms move apart on the surface, forming well-defined structures. The alkali ↔ alkali repulsion also affects the adsorption energy of the alkali.[4] Our results for Cs/Al_2O_3 and data for Cs/TiO_2(110)[4a,38] show a reduction of 30−45 kcal/mol in the adsorption energy of cesium when one goes from systems with low coverage to a saturated adlayer of cesium.

Silver and zinc do not wet the surface of alumina well and form 3D clusters or particles. This behavior is similar to that reported for Cu, Pt, Pd, and Rh films supported on α-Al_2O_3(0001).[5,17] In the case of silver, such a behavior is not surprising, since the metal, in general, has a low affinity toward oxygen.[19,35a] On the other hand, the behavior of zinc is difficult to explain because this metal forms stable oxides[19] with a stability comparable to that of cesium oxides.[42] Previous studies investigating the interaction of a series of metals with TiO_2(110) show that the wetting ability of the admetal increases when its affinity toward oxygen rises.[15] Thus, admetals that form oxides with heats of formation similar to those of zinc oxides (Na, Cs, Fe, Mn) wet the TiO_2(110) surface, whereas poor wetting is observed for the deposition of metals that form oxides with relatively small heats of formation (Cu, Pd, Pt, Au).[4,15]

To explain the differences in the behavior of the Cs/alumina and Zn/alumina systems, one must consider differences in the surface free energy of the admetals and in the nature of the admetal−oxide bonds. In principle, the adhesion energy (E_{adh}) of a metal on an oxide is given by[4,11c]

$$E_{adh} = \gamma_{metal} + \gamma_{oxide} - \gamma_{metal/oxide}$$

where γ_{metal} and γ_{oxide} are the surface energies of the metal and oxide, respectively, and $\gamma_{metal/oxide}$ is the metal/oxide interfacial energy. If $-\gamma_{metal/oxide} > \gamma_{metal} - \gamma_{oxide}$, then the metal will wet the oxide surface.[4] Since the surface energy of metals is usually larger than that of oxides,[51] there must be very good bonding at the metal/oxide interface for wetting to occur.[4] Cesium exhibits a extremely low surface energy (0.07 J m^{-2} [52]), which is much smaller than those of alumina (0.9 J m^{-2} [51]), zinc (0.94 J m^{-2} [52]), and silver (1.30 J m^{-2} [52]). Thus, on the basis of differences in surface free energy, the wetting ability of the admetals investigated in this work should follow the order Ag < Zn < Cs. In the cases of Ag and Zn, wetting will be highly dependent on the strength of the Ag−Al_2O_3 and Zn−Al_2O_3 bonds.

In Figure 11, we compare the relative positions of the valence s orbitals of Cs, Ag, and Zn with respect to the bands of alumina.

The results for alumina come from band-structure calculations,[53] while the position of the Cs(6s), Ag(5s), and Zn(4s) orbitals was estimated using experimental atomic ionization potentials.[54] In alumina the O 2p band is fully occupied, the Al 3s,p band is empty, and there are unoccupied surface states ("SS" in Figure 11) within the bandgap.[53,55] For atomic Zn the valence s shell is completely filled, whereas the corresponding shells of Ag and Cs are only half occupied.[56] Theoretical studies examining the adhesion of 3d transition metals on alumina surfaces[8] have identified two band−orbital interactions responsible for the adhesion strength of the metals. Alumina(O 2p)−metal(3d) repulsive closed-shell interactions were found to be a destabilizing factor, while alumina(Al 3s,p)−metal(3d) charge-transfer interactions favored interface formation.[8] We will analyze the $Cs-Al_2O_3$, $Ag-Al_2O_3$, and $Zn-Al_2O_3$ bonds according to this line of thought.

The valence s orbitals of Cs are much less stable than those of Ag or Zn (see Figure 11). This favors "charge-transfer interactions" between the Cs(6s) orbitals and the empty surface states or bands of alumina, making the $Cs-Al_2O_3$ bond stronger than the $Ag-Al_2O_3$ and $Zn-Al_2O_3$ bonds. For the alumina(O 2p)−metal(s) repulsive interactions, the occupancy of the s shell of the admetal is critical. The alumina(O 2p)−metal(s) interactions produce bonding and antibonding bands (see right side of Figure 11). In the case of Zn/alumina the antibonding band is fully occupied, making the alumina(O 2p)−metal(s) repulsive interactions larger in this system than in the Cs/alumina and Ag/alumina systems. Thus, the small sticking coefficient of Zn on alumina surfaces and the poor wetting in Zn/alumina systems are probably a consequence of weak alumina(SS/Al 3s,p)−Zn(4s) attractive interactions and strong alumina(O 2p)−Zn(4s) repulsive closed-shell interactions. On the other hand, for Cs/alumina, there are strong alumina(SS/Al 3s,p)−Cs(6s) attractive interactions plus relatively weak alumina(O 2p)−Cs(6s) repulsive interactions, and the result is a strong admetal−oxide bond and substantial changes in the electronic properties of alumina.

Small silver clusters deposited on alumina show Ag 3d and 4d binding energies larger (0.4−0.6 eV) than those of pure metallic silver. At the same time, the supported silver clusters exhibit a narrower valence d band. Similar electronic perturbations have been reported for platinum clusters supported on alumina.[12a] In these systems, the limited Ag ↔ Ag and Pt ↔ Pt interactions lead to an incompletely developed metallic band structure for the small Ag and Pt clusters. In the Ag/alumina and Pt/alumina surfaces,[7b,12a] the presence of oxygen (or O−Al bonds) prevents strong Ag ↔ Al and Pt ↔ Al interactions, and one sees electronic perturbations in the admetals that are much smaller than those seen after depositing Ag and Pt on clean aluminum surfaces, where core- and valence-level shifts on the order of 0.8−1.4 eV have been found.[32,57] The results of ab initio SCF cluster calculations for Ag/Al(111) and Pt/Al(111) surfaces,[58] plus L-edge XANES (X-ray absorption near-edge structure) measurements for bulk alloys,[59] show a reduction in the population of the Ag(4d) and Pt(5d) bands (0.1−0.35 electron) as a result of bimetallic bonding. The key that makes possible these electronic perturbations is the existence of a stable and almost empty valence band in metallic aluminum.[58] A band with these properties is not present in alumina, and recent ab initio SCF calculations dealing with the interaction of Ag and Pt atoms with $\{Al_mO_n\}^{3m-2n}$ clusters show only small changes (0.02−0.08 electron) in the Ag(4d) and Pt(5d) populations.[60]

V. Conclusions

(1) In the Cs/alumina systems the alkali atoms wet the oxide, forming strong chemisorption bonds. As the Cs coverage increases, there is a reduction in the Cs desorption temperature from 1000 to 300 K. This reflects a continuous decrease in the Cs adsorption energy from 63 to 18 kcal/mol. The deposition of small amounts of Cs induces large (0.9−1.1 eV) shifts in the binding energies of the O KVV, O 1s, and Al 2p features of alumina. This is consistent with a transfer of electrons from Cs into surface states of alumina that produces a transformation similar to a change from p-type to n-type semiconductors.

(2) Silver does not wet the surface of alumina well and prefers to form 3D clusters on this oxide. Small silver clusters supported on alumina show Ag 3d and 4d binding energies larger (0.4−0.6 eV) than those of pure metallic silver. At the same time, the clusters exhibit a narrower valence d band. The deposition of silver induces only minor perturbations in the electronic properties of alumina.

(3) Despite the large stability of compounds between zinc and oxygen, the interactions between zinc and alumina are weak. At room temperature, the sticking coefficient of zinc on alumina is negligible. In the Zn/alumina systems, the wetting of the oxide surface is poor and the admetal forms 3D clusters. The activation energy for desorption of Zn increases with cluster size varying in the range from 20 to 30 kcal/mol.

Acknowledgment. The authors thank C. T. Campbell for helpful discussions and sending unpublished papers. This work was carried out at Brookhaven National Laboratory and supported by the U.S. Department of Energy, Division of Chemical Sciences (DE-AC02-76CH00016).

References and Notes

(1) Satterfield, C. N. *Heterogeneous Catalysis in Industrial Practice*, 2nd ed.; McGraw-Hill: New York, 1991.

(2) Bond, G. C. *Heterogeneous Catalysis*; Oxford: New York, 1987.

(3) Henrich, V. E.; Cox, P. A. *The Surface Science of Metal Oxides*; University Press: Cambridge, 1994.

(4) (a) Campbell, C. T. *J. Chem. Soc., Faraday Trans.* **1996**, *92*, 1435. (b) Campbell, C. T. *Surf. Sci. Rep.*, in press.

(5) (a) Goodman, D. W. *Chem. Rev.* **1995**, *95*, 523. (b) Xu, X.; Vesecky, S. M.; Goodman, D. W. *Science* **1992**, *258*, 788. (c) Xu, X.; Goodman, D. W. *J. Phys. Chem.* **1993**, *97*, 7711. (d) Xu, X.; Chen, P.; Goodman, D. W. *J. Phys. Chem.* **1994**, *98*, 9242. (e) Coulter, K.; Xu, X.; Goodman, D. W. *J. Phys. Chem.* **1994**, *98*, 1245. (f) Wu, M.-C.; Oh, W. S.; Goodman, D. W. *Surf. Sci.* **1995**, *330*, 61.

(6) Ludviksson, A.; Ernst, K. H.; Zhang, R.; Yoshihara, J.; Campbell, C. T. *Phys. Rev. B* **1993**, *47*, 13782.

(7) (a) Venus, D.; Hensley, D. A.; Kesmodel, L. L. *Surf. Sci.* **1988**, *199*, 391. (b) Fritsch, A.; Légaré, P. *Surf. Sci.* **1987**, *184*, L355. (c) Bastl, Z. *Vacuum* **1986**, *36*, 447.

(8) Alemany, P.; Boorse, R. S.; Burlitch, J. M.; Hoffmann, R. *J. Phys. Chem.* **1993**, *97*, 8464.

(9) (a) Freund, H.-J.; Kuhlenbeck, H.; Staemmler, V. *Rep. Prog. Phys.* **1996**, *59*, 283. (b) Iwasawa, Y. *Stud. Surf. Sci. Catal.* **1996**, *101*, 21.

(10) (a) Beitel, G.; Markert, K.; Wiechers, J.; Hrbek, J.; Behm,R. J. In *Adsorption on Ordered Surfaces of Ionic Solids and Thin Films*; Umbach, E., Freund, H. J., Eds; Springer-Verlag: Berlin, 1993; pp 71−82. (b) Van Campen, D. G.; Hrbek, J. *J. Phys. Chem.* **1995**, *99*, 16389.

(11) (a) Zhou, J. B.; Lu, H. C.; Gustafsson, T.; Garfunkel, E. *Surf. Sci.* **1993**, *293*, L887. (b) Didier, F.; Jupille, J. *Surf. Sci.* **1994**, *307−309*, 587. (c) Didier, F.; Jupille, J. *Surf. Sci.* **1994**, *314*, 378.

(12) (a) Altman, E. I.; Gorte, R. J. *Surf. Sci.* **1989**, *216*, 386. (b) Roberts, S.; Gorte, R. J. *J. Chem. Phys.* **1990**, *93*, 5337. (c) Zafiris, G. S; Gorte, R. J. *J. Catal.* **1993**, *139*, 561. (d) Cordatos, H.; Bunluesin, T.; Stubenrauch, J.; Vohs, J. M.;Gorte, R. J. *J. Phys. Chem.* **1996**, *100*, 785.

(13) Petrie, W. T.; Vohs, J. M. *J. Chem. Phys.* **1994**, *101*, 8098.

(14) (a) Wu, M.-C.; Møller, P. J. *Phys. Rev. B* **1989**, *40*, 6063. (b) Wu, M.-C.; Møller, P. J. *Surf. Sci.* **1989**, *224*, 250.

(15) (a) Steinrück, H.-P.; Pesty, F.; Zhang, L.; Madey, T. E. *Phys. Rev. B* **1995**, *15*, 2427. (b) Pan, J.-M.; Maschoff, B. L.; Diebold, U.; Madey, T. E. *Surf. Sci.* **1993**, *291*, 381. (c) Diebold, U.; Pan, J.-M.; Madey, T. E. *Phys. Rev. B* **1993**, *47*, 3868. (d) Pan, J.-M.; Madey, T. E. *J. Vac. Sci. Technol. A* **1993**, *11*,1667.

(16) Prabhakaran, K.; Purdie, D.; Casanova, R.; Muryn, C. A.; Hardman, P. J.; Wincott, P. L.; Thornton, G. *Phys. Rev. B* **1992**, *45*, 6969.

(17) (a) Cordatos, H.; Bunluesin, T.; Gorte, R. J. *Surf. Sci.* **1995**, *323*, 219. (b) Altman, E. I.; Gorte, R. J. *J. Catal.* **1988**, *113*, 185. (c) Altman, E. I.; Gorte, R. J. *J. Catal.* **1988**, *110*, 191.

(18) (a) Zomerdijk, J. C.; Hall, M. W. *Catal. Rev. Sci. Eng.* **1981**, *23*, 163. (b) Van Santen, R. A.; Kuipers, H. P. C. E. *Adv. Catal.* **1987**, *35*, 265.

(19) *Handbook of Chemistry and Physics*, 58th ed.; Weast, R. C., Ed.; CRC Press: Cleveland, OH, 1977; pp D-70, D-75, D-78.

(20) (a) Wu, M.-C.; Estrada, C. A; Goodman, D. W. *Phys. Rev. Lett.* **1991**, *67*, 2910. (b) Truong, C. M.; Wu, M.-C.; Goodman, D. W. *J. Chem. Phys.* **1992**, *97*, 9447.

(21) Chen, P. J.; Colaianni, M. L.; Yates, J. T. *Phys. Rev. B* **1990**, *15*, 8025.

(22) Williams, G. P. *Electron Binding Energies of the Elements*, Version II; National Synchrotron Light Source, Brookhaven National Laboratory: Upton, NY, 1992.

(23) Kuhn, M.; Rodriguez, J. A. *Surf. Sci.* **1996**, *355*, 85.

(24) Wu, Y.; Tao, H.-S.; Garfunkel, E.; Madey, T. E.; Shinn, N. D. *Surf. Sci.* **1995**, *336*, 123.

(25) Cocke, D. L.; Johnson, E. D.; Merrill, R. P. *Catal. Rev. Sci. Eng.* **1984**, *26*, 163.

(26) Rodriguez, J. A.; Kuhn, M. *J. Phys. Chem.* **1995**, *99*, 9567.

(27) Kuhn, M.; Rodriguez, J. A. *Surf. Sci.* **1995**, *336*, 1.

(28) Bauer, E.; Poppa, H. *Thin Solid Films* **1984**, *121*, 159.

(29) (a) The chemisorbed layer of oxygen was prepared according to the procedure described in ref 29b. It probably consisted of oxygen atoms adsorbed on quasi-3-fold hollow and a-top sites of the Mo(110) substrate.[29b] (b) Colaianni, M. L.; Chen, J. G.; Weinberg, W. H.; Yates, J. T. *Surf. Sci.* **1992**, *279*, 211.

(30) Masel, R. I. *Principles of Adsorption and Reaction on Solid Surfaces*; Wiley: New York, 1996; pp 538−540.

(31) Schön, G. *Acta Chem. Scand.* **1973**, *27*, 2623.

(32) Egelhoff, W. F. *Appl. Surf. Sci.* **1982**, *11/12*, 761.

(33) Egelhoff, W. F. *Surf. Sci. Rep.* **1987**, *6*, 253.

(34) Hüfner, S.; Wertheim, G. K.; Wernick, J. H. *Phys. Rev. B* **1973**, *8*, 4511.

(35) (a) Rodriguez, J. A.; Hrbek, J. *J. Phys. Chem.* **1994**, *98*, 4061. (b) Rodriguez, J. A.; Hrbek, J.; Kuhn, M.; Sham, T. K. *J. Phys. Chem.* **1993**, *97*, 4737.

(36) (a) Hrbek, J. *Surf. Sci.* **1985**, *164*, 139. (b) Rodriguez, J. A.; Clendening, W. D.; Campbell, C. T. *J. Phys. Chem.* **1989**, *93*, 5238. (c) Gerlach, R. L.; Rhodin, T. N. *Surf. Sci.* **1970**, *19*, 403. (d) Campbell, C. T. *J. Phys. Chem.* **1985**, *89*, 5789.

(37) (a) These adsorption energies were estimated using Redhead's equation for first-order desorption kinetics[37] with a pre-exponential factor of 10^{13} s^{-1}, a heating rate of 5 K/s, and desorption temperatures of 300 and 1000 K. (b) Redhead, P. A. *Vacuum* **1962**, *12*, 203.

(38) Grant, A; Campbell, C. T. To be published.

(39) Bonzel, H. P. *Surf. Sci. Rep.* **1988**, *8*, 43.

(40) Yang, Y. W.; Hrbek, J. *J. Phys. Chem.* **1995**, *99*, 3229.

(41) Rodriguez, J. A.; Hrbek, J.; Yang, Y.-W.; Kuhn, M.; Sham, T. K. *Surf. Sci.* **1993**, *293*, 260.

(42) The heats of formation of zinc oxide (−83.2 kcal/mol[19]) and cesium oxides (Cs_2O, $\Delta H_f = -75.9$ kcal/mol; C_2O_2, $\Delta H_f = -96.2$ kcal/mol[19]) are similar. ZnO_x and CsO_x films supported on Ru(001) decompose in the same range of temperature: 700−1000 K.[40,43]

(43) Rodriguez, J. A. *J. Phys. Chem.* **1993**, *97*, 6509.

(44) Rodriguez, J. A.; Kuhn, M. *J. Phys. Chem.* **1996**, *100*, 381.

(45) These energies were calculated using the Redhead's equation for first-order desorption kinetics[37b] with a pre-exponential factor of 10^{13} s^{-1}, a heating rate of 5 K/s, and desorption temperatures of 375 ($\theta_{Zn} = 0.3$) and 435 K ($\theta_{Zn} = 4.2$).

(46) Previous studies show a difference of 0.2−0.5 eV between the Zn $2p_{1/2}$ binding energy of zinc oxides and metallic Zn.[43,47]

(47) (a) Wagner, C. D.; Riggs, W. M.; Davis, L. E.; Moulder, J. F.; Muilenberg, G. E. *Handbook of X-ray Photoelectron Spectroscopy*; Perkin-Elmer: Eden Praire, MN, 1978. (b) Wagner, C. D.; Gale, L. H.; Raymond, R. H. *Anal. Chem.* **1979**, *51*, 466.

(48) Rodriguez, J. A.; Hrbek, J. *Catal. Lett.* **1994**, *26*, 393.

(49) (a) Hardman, P. J.; Casanova, R.; Prabhakaran, K.; Muryn, C. A.; Wincott, P. L.; Thornton, G. *Surf. Sci.* **1992**, *269/270*, 677. (b) Prabhakaran, K.; Purdie, D.; Casanova, R.; Muryn, C. A.; Hardman, P. J.; Wincott, P. L.; Thornton, G. *Phys. Rev. B* **1992**, *45*, 6969. (c) Purdie, D.; Muryn, C. A.; Crook, S.; Wincott, P. L.; Thornton, G.; Fischer, D. A. *Surf. Sci.* **1993**, *290*, L680. (d) Taylor, P. A.; Hopkins, B. J. *J. Phys. C: Solid State Phys.* **1978**, *11*, L643. (e) Leysen, R.; Hopkins, B. J.; Taylor, P. A. *J. Phys. C: Solid State Phys*. **1975**, *8*, 907.

(50) Onishi, H.; Iwasawa, Y. *Catal. Lett.*, in press.

(51) Overbury, S. H.; Bertrand, P. A.; Somorjai, G. A. *Chem. Rev.* **1975**, *75*, 547.

(52) Mezey, L. Z.; Giber, J, *Jpn. J. Appl. Phys.* **1982**, *21*, 1569.

(53) Ciraci, S.; Batra, I. P. *Phys. Rev. B* **1983**, *28*, 982.

(54) Moeller, T. *Inorganic Chemistry*; Wiley: New York, 1982; pp 77−78.

(55) Causa, M.; Dovesi, R.; Pisani, C.; Roetti, C. *Surf. Sci.* **1989**, *215*, 259.

(56) Emsley, J. *The Elements*; Oxford: New York, 1989.

(57) Rodriguez, J. A.; Kuhn, M. *Chem. Phys. Lett.* **1995**, *240*, 435.

(58) (a) Rodriguez, J. A.; Kuhn, M. *J. Phys. Chem.* **1994**, *98*, 11251. (b) Rodriguez, J. A. *Surf. Sci.* **1996**, *345*, 347.

(59) Jeon, Y.; Chen, J.; Croft, M. *Phys. Rev. B* **1994**, *50*, 6555.

(60) Rodriguez, J. A. To be published. The ab initio SCF calculations were carried out using the effective core potentials and basis sets employed in previous studies on the bonding of Ag and Pt atoms to Al(111).[58] The alumina substrate was modeled using $\{AlO_6\}^{9-}$ and $\{Al_4O_{18}\}^{24-}$ clusters.[61]

(61) (a) Sousa, C.; Illas, F.; Bo, C.; Poblet, J. M. *Chem. Phys. Lett.* **1993**, *215*, 97. (b) Nath, K.; Anderson, A. B. *Phys. Rev. B* **1989**, *39*, 1013.

JP962195W